Macromolecules

ARTICLE

pubs.acs.org/Macromolecules

Visible to Near-IR Electrochromism and Photothermal Effect of Poly(3,4-propylenedioxyselenophene)s

Byeonggwan Kim, Jeonghun Kim, and Eunkyoung Kim*

Active Polymer Center for Pattern Integration, Department of Chemical and Biomolecular Engineering, Yonsei University, 50 Yonsei-ro, Seodaemun-gu, Seoul 120-749, South Korea

Supporting Information

ABSTRACT: A new selenophene derivative, 3,4-propylenedioxyselenophene (ProDOS), was electropolymerized to a polymeric thin film which demonstrated wide spectral tunability from the visible to near-infrared (NIR) region. The anodic and cathodic peaks of the polymeric ProDOS (PProDOS) were observed at +0.22 and −0.30 V, showing a narrow band gap. In the visible region, the PProDOS film showed color change from navy blue in its dedoped state (−0.12 V vs Ag/AgCl) to highly transparent pale gray green in its doped state (0.68 V vs Ag/AgCl) with a high coloration efficiency (CE) of 273 $cm^2\ C^{-1}$ and large transmittance change (contrast ratio of 5.7). The color change of the PProDOS film by electrochromism in the visible region was simultaneously accompanied by NIR electrochromism. Upon exposure to a NIR source (0.7 W cm^{-2}), the doped PProDOS film resulted in a temperature rise of 10.7 °C compared to that of the bare indium tin oxide (ITO) coated glass, while the navy blue colored PProDOS film experienced a temperature rise of 10.2 °C. This photothermal effect by NIR light exposure was switchable between the colored and bleached state by simply dedoping and doping the film electrochemically, respectively. Furthermore, bleached PProDOS particles dispersed in water (0.05 mg mL^{-1}) also showed a high photothermal effect (2 W cm^{-2}) with a temperature rise of 13.1 °C, as compared to pure water. Compared with poly(3,4-ethylenedioxythiophene) (PEDOT), it was found that the new selenophene polymer (PProDOS) provided efficient visible to NIR electrochromism in addition to the high photothermal effect, resulting in a large temperature rise and heat conversion upon exposure to a NIR source.

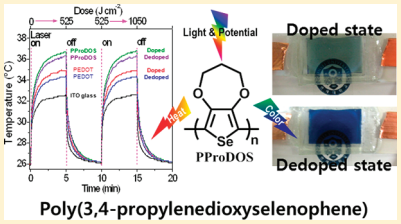

INTRODUCTION

Electroactive polymers from heterocyclic aromatic monomers have received significant attention for applications in electronics such as electrochromic devices (ECDs),[1−10] organic thin film transistors (OTFTs),[11−15] photovoltaic cells,[16−19] organic light-emitting diodes (OLEDs),[20,21] and sensors[22−24] due to their controllable optical and electrical properties by external electrical stimuli. In particular, these heterocyclic electroactive polymers and their derivatives have advantages for use in organic electronics over inorganic materials as they demonstrate a low working voltage, color tunability, and long-term stability with solution processability.[1,25−27] Thus, new materials based on heterocyclic monomers are being actively researched to attain high color contrast, fast response, easy processability, and high sensitivity. Furthermore, it is a challenge to explore bi- or multifunctional electroactive polymers for sensing or imaging. In particular, a combination of electrochromic and photothermal properties could shine light on various electro-optical interests and practical applications including theragnosis based on chromogenic imaging plus near-infrared (NIR) photothermal ablation,[28,29] optical attenuators,[30] night vision sensors,[31] spacecraft thermal controls,[32] and solar cells.[33] Specifically, organic nanoparticles consisting of polyanilines have been used for photothermal ablation of cancer cells utilizing irradiation with NIR.[34] Although several NIR electrochromic materials such as organic ruthenium complexes,[33,35] quinone containing polymers,[36] and aromatic ring containing amine[37] are known, to our surprise, NIR active polymers obtained from heterocylic monomers are rare.[38] As electroactive polymers from thiophenes and selenophenes have high absorbance and good switching properties in both the visible and NIR region,[1,39] they possess great potential to demonstrate visible electrochromism and a photothermal effect under NIR light irradiation.

To date, poly(3,4-alkylenedioxythiophene)s including poly(3,4-ethylenedioxythiophene) (PEDOT) and poly(3,4-propylenedioxythiophene) (PProDOT) have been developed as the most important materials due to their unique electrochromic (EC) properties with fast optical switching behavior (Scheme 1a).[38−42] Replacing the S atoms of poly(3,4-alkylenedioxythiophene)s with Se atoms, which have a larger atomic size, a lower electronegativity, and higher polarizability, results in poly(3,4-alkylenedioxyselenophene)s, which have lower band gap and, thus, a higher coloration efficiency (CE) than polymers containing S atoms (polythiophenes).[39,45−48] According to calculations, the oligo-selenophenes have more of a quinoid character and take more energy to twist the conjugated chains than oligo-thiophenes.[49] The intermolecular Se···Se interactions in the polyselenophenes provide better interchain charge transfer.[45] For these unique properties, polyselenophene

Received: September 14, 2011
Revised: October 8, 2011
Published: October 26, 2011

dx.doi.org/10.1021/ma202094r | Macromolecules 2011, 44, 8791–8797

Scheme 1. (a) Structures of PEDOT, PProDOT, and PEDOS and (b) Synthesis of Monomer and PProDOS

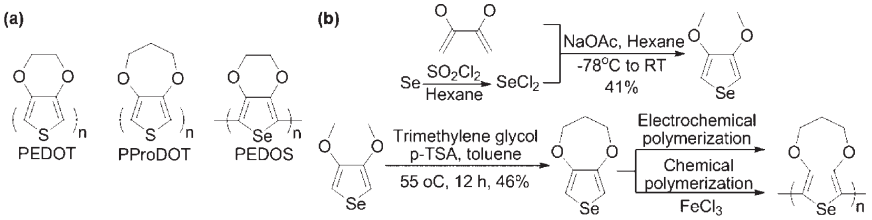

and their derivatives can be used as new EC materials due to their improved optical and electrochemical properties compared to polythiophenes. Poly(3,4-ethylenedioxyselenophene) (PEDOS) is one of the most important polyselenophene derivative for use as a conductive polymer and an EC material.[43] In general, PProDOTs show a higher color contrast with faster EC response than PEDOTs, probably due to the larger degree of freedom necessary for the charge transport in EC reactions in PProDOTs.[43,50] This characteristic can be similarly applied to the selenophene family including poly(3,4-propylenedioxyselenophene) (PProDOS) as a selenophene derivative of PEDOS for tuning the contrast ratio (CR) and electrochromism over a wide spectral range. Therefore, we investigated the synthesis of PProDOS and explored its EC and photothermal properties.

In this paper, we first report the successful synthesis of 3,4-propylenedioxyselenophene (ProDOS) and demonstrate broad range electrochromism of its polymer (PProDOS). We also investigated the unprecedented photothermal properties of PProDOS by irradiating NIR for the first time on heterocyclic conjugated polymers in both a thin film state and with particles in an aqueous media.

EXPERIMENTAL SECTION

General Information. Selenium, sodium acetate (NaOAc), sulfuryl chloride, magnesium sulfate, trimethylene glycol, *p*-toluenesulfonic acid (*p*-TSA), 2,3-butadione, trimethyl orthoformate, sulfuric acid, ammonium dihydrogen phosphate, hydroquinone, absolute methanol, anhydrous hexane, anhydrous toluene, acetonitrile (ACN), and 3,4-ethylenedioxythiophene (EDOT) were purchased from Aldrich. Tetrabutylammonium perchlorate (TBAPC) was purchased from TCI. Indium tin oxide (ITO) coated glass (sheet resistance, R_s = 8−12 Ω sq^{-1}) was purchased from NanoTS Co., Ltd.

Characterization. All electrochemical studies were carried out using a CHI624B (CH Instruments, Inc.) potentiostat using an indium tin oxide (ITO) coated glass as the working electrode, a platinum wire as the counter electrode, and Ag/AgCl wire as the pseudoreference electrode with the supporting electrolyte of 0.1 M TBAPC/ACN. The $E_{1/2}$ = (E_{pa} + E_{pc})/2 of the Fc/Fc^+ couple was 0.36 V vs Ag/AgCl. Electropolymerization of ProDOS was performed on ITO coated glass (0.8 cm × 3 cm) in the supporting electrolyte from a 10 mM monomer and 0.1 M TBAPC/ACN, which was bubbled with N_2 gas for 30 min before use to remove dissolved oxygen. UV-vis-NIR spectra (OPTIZEN 3220UV Spectrophotometer, Mecasys Co., Ltd.) of the PProDOS film on ITO coated glass were obtained as a function of the applied potential while chronoamperometric and absorptiometric experiments of the PProDOS film were monitored at 626 nm and −0.3 to +0.8 V vs Ag/AgCl in a 0.1 M TBAPC/ACN solution. The FTIR spectra of ProDOS and chemically polymerized PProDOS were recorded on a Bruker Tensor 37 FTIR spectrometer with attenuated total reflectance (ATR). The color coordination of the PProDOS film was measured by a colorimeter (color reader CR-10, Konica Minolta Co., LTD). ^{1}H NMR and ^{13}C NMR spectra were recorded utilizing an Unity-Inova NMR (500 and 125 MHz) and Bruker Biospin Avance II (400 and 100 MHz). $CDCl_3$ was used as a solvent with tetramethylsilane (TMS) as an external standard. The chemical shifts (δ) were calculated in units of ppm relative to TMS. Elemental analysis was carried out in an elemental analyzer (FLASH 1112, Thermo Fisher Scientific) using a thermal conductivity detector. Column chromatography was carried out on silica gel (60−230 mesh, Merck) for purification of the products. Toluene was distilled under a dry argon atmosphere and sodium/benzophenone was used as a water absorbent. Anhydrous ACN was degassed under a dry argon atmosphere. TBAPC was dried under vacuum. Ferrocene (Aldrich) was used to establish an electrochemical reference. The average particle sizes of PProDOS and PEDOT were measured by dynamic light scattering (DLS, BI Particle Sizer, ZPA, Brookhaven Instruments Corp.). The field emission scanning electron microscope (FE-SEM) images were obtained by a Hitachi S-4200.

Synthesis. The 3,4-propylenedioxyselenophene (ProDOS) monomer was synthesized from 3,4-dimethoxyselenophene, which was obtained from 2,3-dimethoxybuta-1,3-diene[51] in two steps from 2,3-butadione (Scheme 1b).

Synthesis of 3,4-Dimethoxyselenophene. Selenium dichloride ($SeCl_2$) was prepared in the solution state by adding sulfuryl dichloride (SO_2Cl_2) (14.2 g, 105 mmol) to selenium (8.30 g, 105 mmol) at 10 °C. After 30 min, 30 mL of hexane was added to the mixture and the solution mixture was stirred for 12 h at room temperature. Then, $SeCl_2$ was formed in the clear reddish brown solution. The solution of $SeCl_2$ was added to a well packed and stirred mixture of 2,3-dimethoxy-1,3-butadiene (10.0 g, 87.6 mmol) and sodium acetate (20.5 g, 250 mmol) in anhydrous hexane (1.5 L) at −78 °C under an argon atmosphere. After 10 min, the temperature of the solution started to increase to room temperature and the inhomogeneous solution was stirred for 3 h. The final mixture was washed with distilled water (500 mL × 2), dried over magnesium sulfate ($MgSO_4$), filtered, and concentrated to obtain a yellow oil. The crude product was purified by column chromatography (hexane) to obtain 3,4-dimethoxyselenophene (6.78 g, 40.5%) as a colorless transparent liquid which crystallized in hexane when kept in a dry ice/acetone bath. ^{1}H NMR (500 MHz, $CDCl_3$, δ): 6.56 (s, 2H, Se), 3.86 (s, 6H, $-CH_3$). ^{13}C NMR (125 MHz, $CDCl_3$, δ): 149.04, 95.98, 57.08.

Synthesis of 3,4-Propylenedioxyselenophene (ProDOS). The synthesis of PProDOS is presented in Scheme 1b. 3,4-Dimethoxyselenophene (2.00 g, 10.47 mmol) was dissolved in dry toluene (300 mL) and then propane-1,3-diol (4.78 g, 62.80 mmol, 6 equiv) and *p*-TSA (300 mg) were added to the solution. The mixture was stirred for 6 h at 55 °C. Toluene was evaporated and washed with distilled water, brine, and distilled water. The mixture was extracted with ethyl ether (150 mL × 3) and then concentrated. The crude product was purified by column silica gel chromatography (PE:EE=2:1) and concentrated to obtain 0.967 g of white crystals at a yield of 45.5%.^{1}H NMR (500 MHz, $CDCl_3$, δ): 7.03 (s, 2H, Se), 4.08 (t, 4H, $-O-CH_2-$), 2.19 (m, 2H, $-CH_2-$). ^{13}C NMR (125 MHz, $CDCl_3$, δ): 151.60, 109.08,

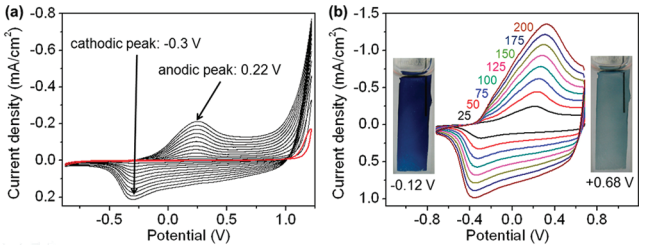

Figure 1. (a) Cyclic voltammogram of the electropolymerization of ProDOS on an ITO coated glass in an ACN solution containing 0.1 M TBAPC and 10 mM monomer, using a platinum wire at a scan rate of 50 mV s^{-1} (vs Ag/AgCl) for 15 cycles. The red line shows the first scan CV. (b) CVs of PProDOS in monomer-free 0.1 M TBAPC/ACN at different scan rates ranging from 25 to 200 mV s^{-1}. (Inset) Photographic images of an electropolymerized PProDOS film on ITO coated glass in its dedoped state (−0.12 V) and doped state (0.68 V).

70.96, 33.73. Anal. Calcd for $C_7H_8O_2Se$: C, 41.40; H, 3.97; O, 15.76. Found: C, 41.48; H, 4.00; O, 15.91.

Preparation and Measurement of Photothermal Switching Effect. PProDOS and PEDOT films were prepared on ITO coated glass with thicknesses of 100 nm by electrochemical polymerization. Voltages of −0.5 and +1.0 V were applied to the films to obtain dedoped (reduced and colored state) and doped films (oxidized and bleached state), respectively. The films were loaded onto a sample holder, which was directly contacted with a thermocouple but separated from the NIR coherent diode laser (808 nm, 50 mW, beam size of 7 mm^2, B&W Tek, Inc.). The temperature of the sample was directly measured by a thermocouple (TES2732, Multimeter) with a minimum detection time of 1 s and a minimum threshold of 0.1 °C. No electrical current was flown through the film during the temperature measurements.

To measure the photothermal effect of PProDOS and PEDOT particles in water, bleached and colored polymer particles were collected from the detached film from the ITO coated glass after the electrochemical doping (at 1.0 V) and dedoping processes (at −0.5 V), respectively. The collected particles were filtered to remove large particles and dispersed in water. Then, the solution was sonicated. The clear supernatant of the solutions was collected and the large particles were removed by filtration using a membrane (pore size <1 μm). The average particle sizes (size distribution, PDI) of PProDOS (dedoped), PProDOS (doped), PEDOT (dedoped), and PEDOT (doped) were 167 nm (0.22), 173 nm (0.37), 187 nm (0.87), and 204 nm (0.43), respectively, with relatively broad particle size distributions. The dried PProDOS and PEDOT particles were weighed by a microbalance (Sartorius CPA2P, resolution of 0.001 mg) and put into distilled water at a concentration of 0.05 mg mL^{-1}. Each solution of doped and dedoped polymeric particles was added to flat-bottom glassware and a NIR coherent diode laser (808 nm, 140 mW, beam size of 7 mm^2, B&W Tek, Inc.) was exposed to the center of the sample. The temperature of the sample was directly measured by a thermocouple (Fluke 287, multimeter) with a minimum detection time of 1 s and a minimum threshold of 0.1 °C.

RESULTS AND DISCUSSION

Electrochemical Properties of PProDOS. The cyclic voltammogram (CV) of the solution containing ProDOS monomer initially showed a broad irreversible anodic peak beyond 1.2 V (vs Ag/AgCl) (Figure 1a, red line), corresponding to the oxidation of the monomer. During repetitive cycling within the potential range from −0.9 to +1.2 V, the CV of the solution showed new anodic and cathodic peaks at +0.22 and −0.30 V, respectively, with the deposition of a dedoped polymeric film (Figure 1a). Those peaks are characteristic of the redox peak for PProDOS, where the reduction peak for PProDOS was shifted toward a more positive value than the peak of the PEDOS film,[47] as similarly observed for the PEDOT and PProDOT couple (Table 1). These results indicate that the additional methylene group in PProDOS facilitates the dedoping process, as previously discussed in the literature.[50] Furthermore, the half-wave reduction potential ($E_{1/2}$) was shifted toward a more positive value than the peak of the S atom analogue (PProDOT) film, indicating that the reduction process is further facilitated by the presence of large Se atom.

Figure 1b shows the CVs of a 100 nm thick PProDOS film at different scan rates. The anodic and cathodic current densities (j_p) at the peak potentials were linearly correlated to the square root of the scan rate ($v^{1/2}$) with the PProDOS film (Figure 2) with a correlation constant of R^2=0.995. The counterion diffusion coefficients of the doping/dedoping process of PProDOS were obtained from the linear relationship of the anodic current density (j_{pa}) and cathodic current density (j_{pc}) as a function of $v^{1/2}$ according to the Randles−Sevcik equation[52]

$$j_p = 0.4463nFC(nFvD_f/RT)^{1/2} \quad (1)$$

where j_p, C, n, F, v, D_f, R, and T are the peak current density (A cm^{-2}), the concentration of electrolyte solution (mol cm^{-3}), the number of electrons transferred in the redox event, the Faraday constant (C mol^{-1}), the scan rate (V s^{-1}), the diffusion coefficient of the counterion (cm^2 s^{-1}), the ideal gas constant (J K^{-1} mol^{-1}), and the temperature (K), respectively. The D_f of the PProDOS film were determined to be 2.06×10^{-8} cm^2 s^{-1} and 1.08×10^{-8} cm^2 s^{-1} under doping and dedoping, respectively. A slower dedoping process than doping process is common for polythiophenes and their derivatives and attributed to the dense doped polymer film.[3,44] The D_f difference between doping and dedoping process, originated from the difference in the surface strucutre, was matched to the surface morphology examined by a FE-SEM (Figure 6).

Electrochromic (EC) Properties of PProDOS. The dedoped and doped state PProDOS film exhibited $L^*a^*b^*$ color coordinates of 46.6, 8.8, and −18.7 and 65.2, −6.3, and −12.4, respectively. The color index $E = (L^{*2} + a^{*2} + b^{*2})^{1/2}$, chroma $C^* = (a^{*2} + b^{*2})^{1/2}$, and hue angle $h^0 = \arctan(b^*/a^*)$ were determined using CIELAB. The doped PProDOS film showed a higher E index value of 66.7 than the dedoped film (50.9), indicating a higher brightness in the doped state. The chroma (C^*) value of the doped PProDOS film (13.8) was closer to gray ($a^* = b^* = 0$) than that of the dedoped film (20.6). The hue angle values also matched observations with the naked eye, in both the dedoped (295°) and doped states (63°).

Figure 3a shows the EC properties of the PProDOS film evaluated by in situ collection of UV−vis−NIR absorbance spectra as a function of the applied potential between −0.12 and +0.68 V. The absorption max (λ_{max}) for the PProDOS film in the dedoped state was observed at 626 nm and consisted of two shoulder bands (Table 1), which is characteristic of a multiple $\pi-\pi^*$ electronic transition. Such vibronic bands can be attributed to the conjugation of the lone pair electrons of Se atoms with neighboring π-bondings.[39,47] Importantly, within the small potential difference, the PProDOS film exhibited a full spectral change from the dedoped to doped state, whereas a PEDOS film requires a larger potential difference, −1.3 V and +0.6 V.[45]

Table 1. Comparison of the Electrochemical and Optical Properties of PProDOS with PProDOT, PEDOS, and PEDOT

	E_{onset}[a] (V)	$E_{1/2}$[b] (V)	l_{max}[c] (nm)	l_{middle}[d] (nm)	E_g[e] (eV)	ΔT[f] (%)	CE[g] (cm^2 C^{-1})	switching time[i] (s)	ref
PProDOS	−0.33	−0.04	626	686	1.65	51	273 (241)[h]	0.86 (0.66)[j]	this work
PProDOT	−0.35	−0.12	567	625	1.7	54	255	0.95	41, 42
PEDOS	−0.95	−0.49	666	-	1.42	55	212	0.6[j]	43, 44
PEDOT	−0.97	−0.58	585	-	1.6	54	183	0.75	38−41

[a] The onset of the reduction potential of the polymer film. [b] The half-wave reduction potential $E_{1/2} = (E_{pa} + E_{pc})/2$. [c] The maximum absorbance peak value of the extreme dedoped polymer film. [d] The shoulder absorbance peak value of the extreme dedoped polymer film. [e] The optical band gap calculated from the onset absorbance of the $\pi-\pi^*$ transition of the polymer in the dedoped state. [f] The transmittance difference between the doped state (T_{dop}) and dedoped state (T_{de}). [g] The coloration efficiency at 95% of full switch. [h] The coloration efficiency at full switch. [i] The essential time for switching the doped state of the polymer film from the dedoped state to the oxidation state at full switch. [j] The time for switching the doped state of the polymer film from the dedoped state to the oxidation state at 95% of full switch.

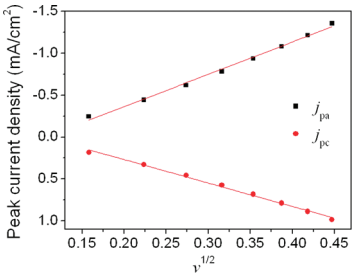

Figure 2. Anodic and cathodic peak current density as a function of the square root of scan rate for a PProDOS film in 0.1 M TBAPC/ACN solution.

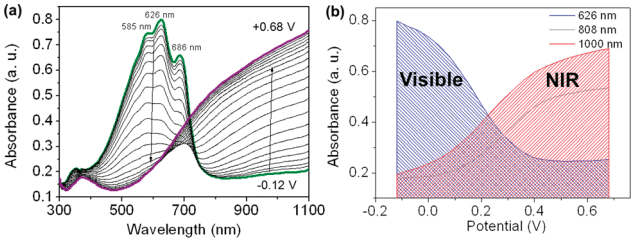

Figure 3. (a) *In situ* spectroelectrochemistry of a PProDOS film prepared on ITO coated glass as a function of the applied potential between −0.12 and +0.68 V vs Ag/AgCl at intervals of 40 mV in a 0.1 M TBAPC/ACN supporting electrolyte using a platinum wire as the counter electrode. The absorbance data was obtained after the polymer film was fully equilibrated at the applied potential for 10 s. (b) Absorbance changes at 626, 808, and 1000 nm in part a as a function of the applied potential between −0.12 and +0.68 V.

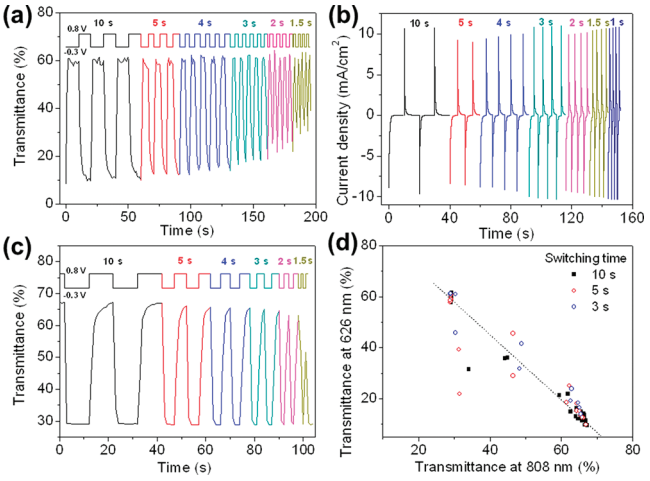

Figure 4. (a) Transmittance changes determined by chronoabsorptometric measurements in the visible range monitored at 626 nm in response to potential-step chronoamperometry between −0.3 and +0.8 V vs Ag/AgCl in a 0.1 M TBAPC/ACN solution electrolyte with switching times of 10, 5, 4, 3, 2, and 1.5 s. (b) Chronoamperometric response observed in part a. (c) Transmittance changes determined by chronoabsorptometric measurements in the NIR range monitored at 808 nm in response to potential-step chronoamperometry between −0.3 and +0.8 V vs Ag/AgCl in a 0.1 M TBAPC/ACN solution electrolyte with different switching times of 10, 5, 4, 3, 2, and 1.5 s. (d) Response of the transmittance vs the step potential in the visible range (626 nm) obtained from part a and the NIR range (808 nm) obtained from part c with different switching times of 10 s (black square), 5 s (red open circle), and 3 s (blue open circle).

Furthermore, the EC transition of PProDOS in the visible range was accompanied by a huge spectral change in the NIR range with an isosbestic point at ∼718 nm. Figure 3b shows the evolution of the NIR absorption in response to applied potentials at the expense of visible absorption, indicating that the visible and NIR electrochromism could be conveniently controlled by the applied potential in the PProDOS film.

As the color change originates from the visible range electrochromism, the EC response of the PProDOS film was determined by monitoring the transmittance change at 626 nm in response to potential step chronoamperometry (Figure 4a). The PProDOS film exhibited a large transmittance change from doped state (T_{dop} = 10.8%) to dedoped state (T_{de} = 61.7%), representing a contrast ratio (CR) of 5.7. The CR value decreased to a shorter residual time, mainly due to slow coloration, while the current response to the step potentials was constant at different switching times (Figure 4b). The EC transmittance response time was 0.6 s for 95% of full switching for doping process. The reverse response time for coloration was longer than that of the doping process (∼6 s). A slow response for coloration is common for conducting polymers based on thiophene[43,44] and is possibly due to the difficulty in counterion diffusion out of the dense polymer film, as demonstrated by the diffusion coefficient determined above from the CV experiments. The coloration efficiency (CE, cm^2 C^{-1}) was determined from the optical change under a given charge density (Q_d, mC cm^{-2}) using the following equation[1]

$$CE = \frac{\Delta OD}{Q_d} = \frac{\log[T_{dop}/T_{de}]}{Q_d} \quad (2)$$

where ΔOD is the optical density change. The CE for the PProDOS film was 273 cm^2 C^{-1} at 95% of full switching

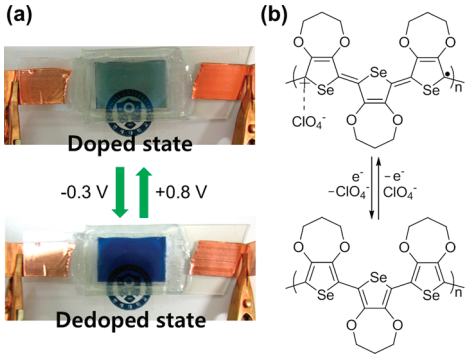

Figure 5. (a) Photographs of the electrochromic device in its extreme states of a transmissive light gray green color at an applied potential of 0.8 V and highly absorbed navy blue color at an applied potential of −0.3 V. (b) Scheme of the doping process of PProDOS in terms of electrochemistry.

(Q_d = 2.70 mC cm^{-2}) (Table 1). This result shows that PProDOS demonstrates highly efficient electrochromism with a small consumption of charge, compared to PProDOT, PEDOT, or PEDOS (Table 1).[44,46]

As shown in Figure 4c, the evolution of transmission in the NIR realm matched well with the decrease in the visible range (Figure 4a), or vice versa, where the NIR transmittance change by the applied potential was monitored at 808 nm. Moreover, the transmittance change in the visible range was linearly correlated to the change in the NIR range (Figure 4d), as presented by eq 3, although there were some outliers at shorter switching values. Such correlation of visible against NIR electrochromism suggests that the NIR properties of PProDOS can be conveniently estimated by the color of the film.

$$T_{vis} = -1.26T_{NIR} + 96(\%) \quad (3)$$

In eq 3, T_{vis} and T_{NIR} are the transmittances in the visible (626 nm) and NIR ranges (808 nm), respectively.

A simple two-electrode ECD was fabricated consisting of a PProDOS film as a working electrode. The two-electrode ECD showed reversible EC switching from a pale gray green color to an intense navy blue color (Figure 5a). The background pattern was clearly readable at +0.8 V but was dramatically hidden at −0.3 V, according to the redox mechanism of PProDOS (Figure 5b). The colored and bleached states remained even after the removal of electricity, demonstrating that PProDOS may be useful as an energy saving display.

Photothermal Properties of the Polymers in Thin Film State. Since PProDOS shows interesting NIR electrochromism, yielding a dramatic absorption increase in the NIR range upon doping, it may be explored as a photothermal material. Thus, the photothermal effect of PProDOS under NIR radiation was examined first in the film state and then with particles in aqueous media as described below (Figure 6a,b). The photothermal effects of the polymeric films were examined by determining their temperature response to 808 nm laser irradiation. Doped and dedoped PProDOS films (100 nm thick each) were prepared electrochemically at +1.0 and −0.5 V, respectively. During the NIR irradiation, there was no noticeable spectral change in either the doped or dedoped state films. The heat evolution is shown in Figure 6a for the doped PProDOS film, which resulted in temperature increases of max. 10.7 ± 0.1 and 4.2 ± 0.1 °C compared to temperatures before NIR exposure and on bare

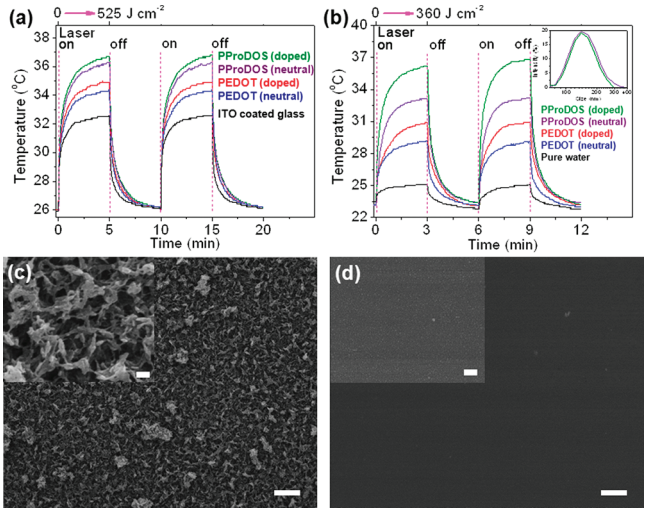

Figure 6. (a) Photothermal effect of the PProDOS and PEDOT films (doped and dedoped states) coated on ITO coated glass along with the bare ITO coated glass by an NIR laser (808 nm, 0.7 W cm^{-2}). The time interval of NIR laser irradiation was 5 min. (b) Photothermal effect of the PProDOS and PEDOT nanoparticles (doped and dedoped state) by an NIR laser (808 nm, 2 W cm^{-2}). The time interval of NIR laser irradiation was 10 min. (Inset) Particle distribution determined from DLS for the doped (olive line) and dedoped (purple line) PProDOS dispersed solutions. FE-SEM images of PProDOS film synthesized by electrochemical polymerization in the (c) dedoped state (−0.5 V) and (d) doped state (1.0 V). The scale bars are 1 μm and 100 nm (inset).

ITO coated glass, respectively (Table 2). The temperature rise from the PProDOS film is remarkable and would be sufficient as a photothermal film for wide applications[53] considering that the photothermal effect in this work was shown in solid state thin films with a small area (7 mm^2). Moreover, the NIR light power used in this work (0.7 W cm^{-2}) is weaker than the light power required for most applications such as 4.5−7 W cm^{-2} for drug delivery application[54] and 2.45 W cm^{-2} for use as a photoablation of cancer cells.[34] Also, the similarity between two cycles of photothermal effect showed that the polymers were stable in NIR laser. This temperature rise by NIR irradiation could be attributed to polarons, which are the charge carriers responsible for the electrical conduction. The temperature rise decreased when the PProDOS film was dedoped. Consequently, the photothermal effect could be electrochemically switched between the doped and dedoped states of PProDOS. It is noteworthy that the dedoped PProDOS film showed a temperature rise of 10.2 ± 0.1 °C upon NIR irradiation. Although it was smaller than that observed for the doped PProDOS film, the significant temperature rise in the dedoped state could be attributed to the rough surface structure of the film. The photothermal effect of the dedoped polymer film is expected to be slight because its absorbance in the NIR range is small (Figure 3a). However, the surface of the dedoped PProDOS film was very rough and composed of 100−300 nm diameter porous agglomerates, as shown in the FE-SEM image in Figure 6c. On the other hand, the surface of the doped PProDOS film was homogeneous (Figure 6d). The pores between the rough and dedoped PProDOS agglomerates are heat insulators which increase temperature of the film higher by NIR irradiation than a dense film without micropores.[55] Moreover, the rough agglomerates could

Table 2. Photothermal Effect of PProDOS and PEDOT

	film state				solution state		
	A_{808}[a] (a.u.)	ΔT_f[b] (°C)	ε_{pt}[c] (K J^{-1})	m_f[d] (μg)	ΔT_s[e] (°C)	d[f] (nm, PDI)	ε_{pt}[g] (K J^{-1})
PProDOS (doped)[h]	0.53	10.7 ± 0.1	0.74	0.36	13.1 ± 0.1	173 (0.37)	0.31
PProDOS (dedoped)[i]	0.18	10.2 ± 0.1	0.69	0.33	9.9 ± 0.1	167 (0.22)	0.20
PEDOT (doped)[h]	0.49	8.9 ± 0.1	0.64	0.34	7.8 ± 0.1	204 (0.43)	0.16
PEDOT (dedoped)[i]	0.20	8.3 ± 0.1	0.6	0.31	6.0 ± 0.1	187 (0.87)	0.14

[a] The absorbance at 808 nm of the film on ITO coated glass. [b] The temperature rise of the polymer film on ITO glass by NIR laser irradiation (0.7 W cm^{-2} for 5 min). [c] The photothermal effect with the dose at the maximum temperature rise (0.7 W cm^{-2} for 10 s) of the polymer film (area: 7 mm^2). [d] The mass of the NIR laser irradiated area of the polymer film (100 nm thick). [e] The temperature rise of the polymer-dispersed water solution by NIR laser irradiation (2 W cm^{-2} for 3 min). [f] The average particle sizes (size distribution, PDI) with relatively broad particle size distributions. [g] The photothermal effect with the dose at the maximum temperature rise (2 W cm^{-2} for 10 s) of the polymer film (area: 7 mm^2). [h] The bleached and colored polymer film or particle after electrochemical doping (at 1.0 V) and [i] dedoping process (at 0.5 V).

enhance light absorption and thus heat generation through scattering of an incident light.[56] Therefore, the dedoped PProDOS film showed higher temperature rise than expected, although its photothermal effect is still lower than the doped one.

The temperature rise of the electrochemically deposited PEDOT film under NIR laser irradiation was also examined under the same conditions. The UV−vis−NIR spectra of the PEDOT films are shown in the Supporting Information. The temperatures of the doped and dedoped PEDOT film increased by 8.9 ± 0.1 °C and 8.3 ± 0.1 °C, compared to temperatures before NIR exposure and on bare ITO glass, respectively. As compared in Figure 6a, the temperature rise for the PEDOT film was less than that of the PProDOS film in both the doped and dedoped states (Table 2).

Photothermal Properties of the Polymer Particles in Solution. To further characterize the photothermal effect in PProDOS by NIR irradiation, we also examined the temperature rise in PProDOS particles dispersed in water and compared the results with PEDOT particles prepared similarly (Figure 6b). Since the quantity of nanoparticles was very small (0.05 mg mL^{-1}), the solutions containing both dedoped and doped particles were transparent (Figure 6b, inset, Supporting Information). Interestingly, when the solutions containing the doped and dedoped PProDOS particles were irradiated by NIR (2 W cm^{-2}), the temperature of the transparent solution was elevated, resulting in temperature increases of 13.1 ± 0.1 °C and 9.9 ± 0.1 °C, respectively, as compared to pure water (2.0 ± 0.1 °C) (Figure 6b). This type of photothermal effect from nanoparticles in aqueous media is beneficial for many biological experiments and can be applied directly for photoablation experiments, which are generally conducted in aqueous media.[34] The temperature of the doped and dedoped PEDOT particles dispersed in water increased by 7.8 ± 0.1 °C and 6.0 ± 0.1 °C, respectively. The temperature rise with the PProDOS particles dispersed in water was larger than in the PEDOT solution, as was similarly observed with the films. Irradiating the polymer with NIR light at a wavelength where the film absorbs light will eventually result in heating of the absorbing layer or particles in solution. Therefore, the larger temperature rise observed with PProDOS compared to PEDOT can be attributed to the larger NIR absorbance (A) of PProDOS (A_{808} = 0.53) than that of PEDOT (A_{808} = 0.49). Moreover, doped conjugated polymers generally show high absorbance in the NIR regions of the spectrum. Thus, the doped samples produced a larger temperature rise when exposed to NIR light than the dedoped samples under the same experimental conditions in both film and particle states. The structural differences at micrometer scale between the doped and dedoped film states (Figure 6c,d) could be minimized in the particle states as the average size of particles is similar for both doped and dedoped particles (167−204 nm) (Figure 6b, inset). Therefore, the photothermal effect difference between the doped and dedoped particles is more pronounced in the nanoparticle solutions, showing much higher temperature increase in the doped state. To our knowledge, this is the first report demonstrating large NIR electrochromism associated with visible electrochromism through a selenophene polymer, which exhibited an interestingly large photothermal effect that could be conveniently detected and switched reversibility by visible electrochromism both the film and particle states. We aware that other factors could affect the photothermal effect including morphology, heat and electron conductivity, and mobility difference between the samples.[57,58] Thus, we hope that further progress in this work will provide details of the photothermal mechanism and application.

CONCLUSIONS

A polymer derived from a new selenophene derivative, ProDOS, was synthesized and its visible to NIR electrochromism behavior along with photothermal effect under NIR light irradiation was investigated. The electrochemically prepared PProDOS film showed visible electrochromism with a high contrast ratio of 5.7 with a fast switching time of 0.6 s and high coloration efficiency of 273 cm^2 C^{-1}. The color change from the visible range electrochromism was accompanied by a NIR range absorption change. PProDOS was demonstrated large photothermal properties to elevate the temperature of the media by 10−13 °C higher under the NIR laser exposure. The temperature rise with PProDOS was always larger than with PEDOT, mainly due to the larger NIR absorbance of ProDOS compared to PEDOT. Moreover, the doped polymers resulted in a larger temperature rise when exposed to NIR light compared to the dedoped polymers, either in the film or particle state. The new selenophene polymer showed an interestingly large photothermal effect that could be conveniently detected and switched reversibility by visible electrochromism in both the film state and the particle state in aqueous media. This behavior may lead to a new realm of organic photothermal materials useful for photoablation therapy and NIR electronics.

ASSOCIATED CONTENT

Supporting Information. UV−vis−NIR spectra of PEDOT film, photographs of the solution containing PProDOS, FTIR

spectra, and NMR spectra of ProDOS and PProDOS and a table of peak assignments for the FTIR spectra. This material is available free of charge via the Internet at http://pubs.acs.org.

AUTHOR INFORMATION

Corresponding Author

*E-mail: eunkim@yonsei.kr. Telephone: +82-2-2123-5752. Fax: +82-2-365-5751.

ACKNOWLEDGMENT

This work was supported by the National Research Foundation (NRF) grant funded by the Korean government (MEST) through the Active Polymer Center for Pattern Integration (No. R11-2007-050-00000-0), the Converging Research Center Program through the Ministry of Education, Science and Technology (2010K001430), and the Pioneer Research Center Program through the National Research Foundation of Korea funded by the Ministry of Education, Science, and Technology (2010-0019313).

REFERENCES

(1) Beaujuge, P. M.; Reynolds, J. R. *Chem. Rev.* **2010**, *110*, 268–320.
(2) Shi, P.; Amb, C. M.; Knott, E. P.; Thompson, E. J.; Liu, D. Y.; Mei, J.; Dyer, A. L.; Reynolds, J. R. *Adv. Mater.* **2010**, *22*, 4949–4953.
(3) Kim, Y.; Kim, Y.; Kim, S.; Kim, E. *ACS Nano* **2010**, *4*, 5277–5284.
(4) Kim, J.; You, J.; Kim, B.; Park, T.; Kim, E. *Adv. Mater.* **2011**, *23*, 4168–4173.
(5) Kim, E.; Jung, S. *Chem. Mater.* **2005**, *17*, 6381–6387.
(6) Baek, J.; Kim, Y.; Kim, E. *J. Nanosci. Nanotechnol.* **2008**, *8*, 4851–4855.
(7) Yun, C.; Seo, S.; Kim, E. *J. Nanosci. Nanotechnol.* **2010**, *10*, 6850–6854.
(8) Kim, J.; Kim, Y.; Kim, E. *Macromol. Res.* **2009**, *17*, 791–796.
(9) Yarimaga, O.; Im, M.; Choi, Y.-K.; Kim, T.; Jung, Y.; Park, H.; Lee, S.; Kim, J.-M. *Macromol. Res.* **2010**, *18*, 404–407.
(10) Ju, Y. W.; Kim, Y. M.; Jung, H. R.; Kim, C.; Yang, K. S.; Lee, W. J. *Appl. Chem.* **2004**, *8*, 502–505.
(11) Zaumseil, J.; Sirringhaus, H. *Chem. Rev.* **2007**, *107*, 1296–1323.
(12) Allard, S.; Forster, M.; Souharce, B.; Thiem, H.; Scherf, U. *Angew. Chem., Int. Ed.* **2008**, *47*, 4070–4098.
(13) Kagan, C. R.; Mitzi, D. B.; Dimitrakopoulos, C. D. *Science* **1999**, *286*, 945–947.
(14) Kim, Y.; Do, J.; Kim, J.; Yang, S. Y.; Malliaras, G. G.; Ober, C. K.; Kim, E. *Jpn. J. Appl. Phys.* **2010**, *49*, 01AE10.
(15) Jo, P.; Park, Y.; Kang, S.; Kim, T.; Park, C.; Kim, E.; Ryu, D.; Kim, H.-C. *Macromol. Res.* **2010**, *18*, 777–786.
(16) Shah, A.; Torres, P.; Tscharner, R.; Wyrsch, N.; Keppner, H. *Science* **1999**, *285*, 692–698.
(17) Thompson, B. C.; Fréchet, J. M. J. *Angew. Chem., Int. Ed.* **2008**, *47*, 58–77.
(18) Koh, J. K.; Kim, J.; Kim, B.; Kim, J. H.; Kim, E. *Adv. Mater.* **2011**, *23*, 1641–1646.
(19) Oh, J.-W.; Choi, J.; Luong, B.; Kim, N. *Macromol. Res.* **2010**, *18*, 8–13.
(20) Burroughes, J. H.; Bradley, D. D. C.; Brown, A. R.; Marks, R. N.; Mackay, K.; Friend, R. H.; Burns, P. L.; Holmes, A. B. *Nature* **1990**, *347*, 539–541.
(21) Kim, J. M.; Song, M. C.; Seol, J. Y.; Hwang, H. M.; Park, C. H. *Korean J. Chem. Eng.* **2005**, *22*, 643–647.
(22) Thomas, S. W.; Joly, G. D.; Swager, T. M. *Chem. Rev.* **2007**, *107*, 1339–1386.
(23) Kim, Y.; Malliaras, G. G.; Ober, C. K.; Kim, E. *J. Nanosci. Nanotechnol.* **2010**, *10*, 6869–6873.
(24) Seo, S.; Kim, J.; Kim, B.; Vinu, A.; Kim, E. *J. Nanosci. Nanotechnol.* **2011**, *11*, 4567–4572.
(25) Roncali, J. *Chem. Rev.* **1997**, *97*, 173–206.
(26) Charvet, R.; Acharya, S.; Hill, J. P.; Akada, M.; Liao, M.; Seki, S.; Honsho, Y.; Saeki, A.; Ariga, K. *J. Am. Chem. Soc.* **2009**, *131*, 18030–18031.
(27) Li, M.; Ishihara, S.; Akada, M.; Liao, M.; Sang, L.; Hill, J. P.; Krishnan, V.; Ma, Y.; Ariga, K. *J. Am. Chem. Soc.* **2011**, *133*, 7348–7351.
(28) Loo, C.; Lowery, A.; Halas, N.; West, J.; Drezek, R. *Nano Lett.* **2005**, *5*, 709–711.
(29) Huang, X.; El-Sayed, I. H.; Qian, W.; El-Sayed, M. A. *J. Am. Chem. Soc.* **2006**, *128*, 2115–2120.
(30) McDonagh, A. M.; Bayly, S. R.; Riley, D. J.; Ward, M. D.; McCleverty, J. A.; Cowin, M. A.; Morgan, C. N.; Varrazza, R.; Penty, R. V.; White, I. H. *Chem. Mater.* **2000**, *12*, 2523–2524.
(31) Sonmez, G.; Schottland, P.; Zong, K.; Reynolds, J. R. *J. Mater. Chem.* **2001**, *11*, 289–294.
(32) Chandrasekhar, P.; Birur, G. C.; Stevens, P.; Rawal, S.; Pierson, E. A.; Miller, K. L. *Synth. Met.* **2001**, *119*, 293.
(33) Schwab, P. F. H.; Diegoli, S.; Biancardo, M.; Bignozzi, C. A. *Inorg. Chem.* **2003**, *42*, 6613.
(34) Yang, J.; Choi, J.; Bang, D.; Kim, E.; Lim, E.-K.; Park, H.; Suh, J.-S.; Lee, K.; Yoo, K.-H.; Kim, E.-K.; Huh, Y.-M.; Haam, S. *Angew. Chem., Int. Ed.* **2011**, *50*, 441–444.
(35) Vickers, S. J.; Ward, M. D. *Electrochem. Commun.* **2005**, *7*, 389–393.
(36) Wang, S.; Todd, E. K.; Birau, M.; Zhang, J.; Wan, X.; Wang, Z. Y. *Chem. Mater.* **2005**, *17*, 6388–6394.
(37) Yen, H.-J.; Liou, G.-S. *Chem. Mater.* **2009**, *21*, 4062–4070.
(38) Franklin, S. R.; Chauhan, P.; Mitra, A.; Thareja, R. K. *J. Appl. Phys.* **2005**, *97*, 094919–4.
(39) Patra, A.; Bendikov, M. *J. Mater. Chem.* **2010**, *20*, 422–433.
(40) Sapp, S. A.; Sotzing, G. A.; Reddinger, J. L.; Reynolds, J. R. *Adv. Mater.* **1996**, *8*, 808–811.
(41) Poverenov, E.; Li, M.; Bitler, A.; Bendikov, M. *Chem. Mater.* **2010**, *22*, 4019–4025.
(42) Bu, H.-B.; Gotz, G.; Reinold, E.; Vogt, A.; Schmid, S.; Blanco, R.; Segura, J. L.; Bauerle, P. *Chem. Commun.* **2008**, 1320–1322.
(43) Kumar, A.; Welsh, D. M.; Morvant, M. C.; Piroux, F.; Abboud, K. A.; Reynolds, J. R. *Chem. Mater.* **1998**, *10*, 896–902.
(44) Gaupp, C. L.; Welsh, D. M.; Rauh, R. D.; Reynolds, J. R. *Chem. Mater.* **2002**, *14*, 3964–3970.
(45) Patra, A.; Wijsboom, Y. H.; Zade, S. S.; Li, M.; Sheynin, Y.; Leitus, G.; Bendikov, M. *J. Am. Chem. Soc.* **2008**, *130*, 6734–6736.
(46) Li, M.; Patra, A.; Sheynin, Y.; Bendikov, M. *Adv. Mater.* **2009**, *21*, 1707–1711.
(47) Li, M.; Sheynin, Y.; Patra, A.; Bendikov, M. *Chem. Mater.* **2009**, *21*, 2482–2488.
(48) Atak, S.; İçli-Özkut, M.; Önal, A. M.; Cihaner, A. *J. Polym. Sci., Part A: Polym. Chem.* **2011**.
(49) Zade, S. S.; Zamoshchik, N.; Bendikov, M. *Chem.—Eur. J.* **2009**, *15*, 8613–8624.
(50) Welsh, D. M.; Kumar, A.; Morvant, M. C.; Reynolds, J. R. *Synth. Met.* **1999**, *102*, 967–968.
(51) McDonald, E.; Suksamrarn, A.; Wylie, R. D. *J. Chem. Soc., Perkin Trans. 1* **1979**, 1893–1900.
(52) Monk, P. M. S.; Mortimer, R. J.; Rosseinsky, D. R. *Electrochromism: Fundamentals and Applications*. Wiley-VCH Verlag GmbH: New York, 2007; pp 2—21.
(53) Eunjung, K.; Yang, J.; Choi, J.; Suh, J.-S.; Huh, Y.-M.; Haam, S. *Nanotechnology* **2009**, *20*, 365602.
(54) You, J.; Shao, R.; Wei, X.; Gupta, S.; Li, C. *Small* **2010**, *6*, 1022–1031.
(55) Sakulin, V. Y.; Migal', V. P.; Margishvili, A. P.; Skurikhin, V. V. *Refract. Ind. Ceram.* **2004**, *45*, 107–113.
(56) Poruba, A.; Fejfar, A.; Remeš, Z.; Špringer, J.; Vaněček, M.; Kočka, J.; Meier, J.; Torres, P.; Shah, A. *J. Appl. Phys.* **2000**, *88*, 148–160.
(57) Link, S.; El-sayed, M. A. *Int. Rev. Phys. Chem.* **2000**, *19*, 409–453.
(58) Peng, S.; McMahon, J. M.; Schatz, G. C.; Gray, S. K.; Sun, Y. *Proc. Natl. Acad. Sci. U.S.A.* **2010**, *107*, 14530–14534.